

# Interstellar Enolization—Acetaldehyde ( $\text{CH}_3\text{CHO}$ ) and Vinyl Alcohol ( $\text{H}_2\text{CCH}(\text{OH})$ ) as a Case Study

N. Fabian Kleimeier<sup>[a]</sup> and Ralf I. Kaiser<sup>\*[a]</sup>

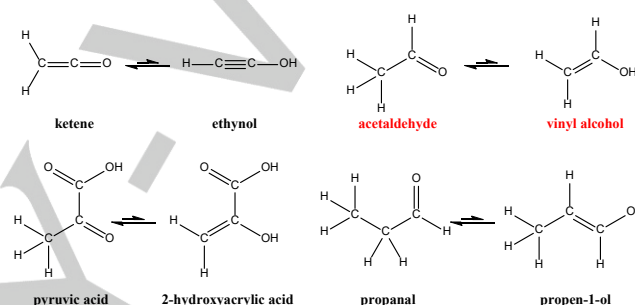
[a] Dr. N. F. Kleimeier and Prof. Dr. R. I. Kaiser  
Department of Chemistry and W. M. Keck Research Laboratory in Astrochemistry  
University of Hawai'i at Manoa  
2545 McCarthy Mall, Honolulu, HI 96822 (USA)  
E-mail: [ralfk@hawaii.edu](mailto:ralfk@hawaii.edu)

**Abstract:** Owing to the unique conditions in cold molecular clouds, enols—the thermodynamically less stable tautomers of aldehydes and ketones—do not undergo tautomerization to their more stable tautomers in the gas phase because they cannot overcome tautomerization barriers at the low temperatures. Laboratory studies of interstellar analog ices have demonstrated the formation of several keto–enol tautomer pairs in astrochemically relevant ice mixtures over the last years. However, so far only one of them, acetaldehyde–vinyl alcohol, has been detected in deep space. Due to their reactivity with electrophiles, enols can play a crucial role in our understanding of the molecular complexity in the interstellar medium and in comets and meteors. To study the enolization of aldehydes in interstellar ices by interaction with galactic cosmic rays (GCRs), we irradiated acetaldehyde ices with energetic electrons as proxies of secondary electrons generated in the track of GCRs while penetrating interstellar ices. The results indicate that GCRs can induce enolization of acetaldehyde and that intra- as well as intermolecular processes are relevant. Therefore, enols should be ubiquitous in the interstellar medium and could be searched for using radio telescopes such as ALMA. Once enols are detected and abundances are established, they can serve as tracers for the non-equilibrium chemistry in interstellar ices thus eventually constraining fundamental reaction mechanisms deep inside interstellar ices.

## Introduction

Complex organic molecules (COM)—per astronomical definition carbon-containing molecules with six or more atoms—make up more than one third of all molecules detected in interstellar and circumstellar environments.<sup>[1]</sup> Laboratory studies and astrochemical modeling demonstrated that the observed abundances of these complex molecules can rarely be explained by gas-phase reactions alone.<sup>[2–3]</sup> Instead, using interstellar analog ices in laboratories, key COMs such as propylene oxide ( $\text{C}_3\text{H}_6\text{O}$ )<sup>[4]</sup> and glycerol ( $\text{CH}_2\text{OHCHOHCH}_2\text{OH}$ )<sup>[5]</sup> have been demonstrated to form efficiently in the solid state upon interaction with photons,<sup>[6–7]</sup> protons,<sup>[8]</sup> and electrons as proxies for galactic cosmic ray interaction with interstellar ices.<sup>[9]</sup> Among the COMs detected in deep space are ketones such as acetone ( $\text{CH}_3\text{COCH}_3$ )<sup>[10]</sup> and aldehydes such as acetaldehyde ( $\text{CH}_3\text{CHO}$ )<sup>[11]</sup> and glycolaldehyde ( $\text{HCOCH}_2\text{OH}$ ),<sup>[12]</sup> often incorrectly referred to in the astronomical community as the

simplest sugar. However, the more reactive tautomers of ketones and aldehydes, i.e. enols, have remained mainly elusive in the interstellar medium. Enols represent reactive intermediates represented by an alkene with a hydroxyl group (OH) attached to the carbon-carbon double bond.



**Scheme 1.** Tautomer pairs observed in different interstellar analog ices subjected to energetic electrons. Tautomer pairs color-coded in red indicate astronomical detections.

Scheme 1 depicts tautomer pairs detected after the processing of interstellar analog ices in the laboratory. Ketene ( $\text{H}_2\text{CCO}$ ) and its ynol, ethynol ( $\text{HCCOH}$ ), have been detected in processed carbon monoxide ( $\text{CO}$ ) - water ( $\text{H}_2\text{O}$ ) ice mixtures,<sup>[13]</sup> whereas carbon monoxide and ethane ( $\text{C}_2\text{H}_6$ ) mixtures yielded propanal ( $\text{CH}_3\text{CH}_2\text{CHO}$ ) and 1-propenol ( $\text{CH}_3\text{CH}=\text{CHOH}$ ).<sup>[14]</sup> Acetaldehyde and vinyl alcohol were detected in ices containing carbon monoxide and methane ( $\text{CH}_4$ )<sup>[14]</sup> or carbon dioxide ( $\text{CO}_2$ ) and ethylene ( $\text{C}_2\text{H}_4$ ),<sup>[15]</sup> and after UV photolysis and proton irradiation of ices containing acetylene ( $\text{C}_2\text{H}_2$ ) and water ( $\text{H}_2\text{O}$ ).<sup>[16]</sup> Furthermore, pyruvic acid ( $\text{CH}_3\text{COCOOH}$ ) and 2-hydroxyacrylic acid ( $\text{CH}_2=\text{COHCOOH}$ ) have been probed in processed acetaldehyde – carbon dioxide ices.<sup>[17]</sup> Other potential candidates for enols in the ISM include 1,1-ethenediol ( $\text{CH}_2=\text{C}(\text{OH})_2$ ) which could form from hydrogenation of ketene,<sup>[18]</sup> and 1-aminoethanol ( $\text{CH}_2=\text{C}(\text{OH})\text{NH}_2$ ), which could form from ketene and ammonia.<sup>[19]</sup> Their tautomers, acetic acid and acetamide, have both been detected in Sgr B2(N)<sup>[20–21]</sup> and the precursors for the formation of 1,1-ethenediol and 1-aminoethanol are readily available in this region. However, so far, the only detected tautomer pair in the interstellar medium is vinyl alcohol ( $\text{CH}_2=\text{CH}(\text{OH})$ )<sup>[22]</sup> –

acetaldehyde in the star forming region SgrB2. As ketones and aldehydes are typically thermodynamically favored over their enol forms, the non-detection might be explained to the novice by their thermodynamic unlikeliness to form, especially at the low temperatures of cold molecular clouds reaching 10 K. However, the non-equilibrium chemistry in interstellar ices driven by energetic radiation such as high energy galactic cosmic ray particles has been demonstrated to yield thermodynamically unfavorable molecules with abundance ratios deviating more than hundred orders of magnitude from their 'expected' thermodynamic equilibrium values.<sup>[14, 23]</sup> Therefore, once formed and released into the gas phase, enols cannot overcome the barrier to tautomerization and hence do not convert back into their more stable aldehyde or ketone form. Consequently, enols play a crucial role in our understanding of the chemical non-equilibrium processes in the extreme environments of the interstellar medium. Once relative abundances of both ketones/aldehydes and their enols are established, they further serve as tracers for non-equilibrium reaction conditions in deep space ultimately refining astrochemical models.<sup>[14]</sup>

A key aspect of enol formation in interstellar model ices that has not yet been adequately addressed is whether they form exclusively during radical-radical recombination processes or if ionizing radiation can induce the enolization in ices containing aldehydes or ketones, i.e. enolization after the formation of aldehydes and/or ketones. A computational investigation suggested that tautomerization of acetaldehyde could proceed via intramolecular enolization through a [1,3]-H shift with a transition state located 277 kJ mol<sup>-1</sup> above acetaldehyde and 236 kJ mol<sup>-1</sup> above vinyl alcohol.<sup>[24]</sup> Previously postulated pathways involving methylhydroxycarbene (CH<sub>3</sub>OCH) as a reactive intermediate have recently been disproved in a matrix isolation study that showed that methylhydroxycarbene exclusively converts into acetaldehyde by [1,2]-H tunneling despite a lower-lying transition state to vinyl alcohol formation.<sup>[24]</sup> Here, exposing ices of pure acetaldehyde—the simplest aldehyde with an  $\alpha$ -hydrogen atom—as a representative example, we investigated the galactic cosmic ray (GCR)-induced enolization of aldehydes in interstellar ices using energetic electrons as a proxy of GCRs.<sup>[25]</sup> The vinyl alcohol formed in these experiments was distinguished from its aldehyde isomer by photoionization reflectron time-of-flight mass spectrometry (PI-ReToF-MS),<sup>[26]</sup> which allowed to exclusively ionize and detect vinyl alcohol. Mechanistic pathways were extracted by exploiting mixtures of acetaldehyde and acetaldehyde-d<sub>4</sub> at cryogenic temperatures in the solid state (5 K)

thus revealing the role of hydrogen-bonded dimers of acetaldehyde in the formation of vinyl alcohol.

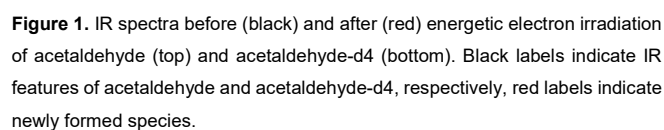
## Results and Discussion

The experiments were conducted for three different ices: pure acetaldehyde, pure acetaldehyde-d<sub>4</sub>, and a 1:1 mixture of both isotopologues. The experimental conditions and the calculated doses received by the ices are summarized in Table 1 and represent model ices exposed to galactic cosmic rays in cold molecular clouds over a time span of a few 10<sup>6</sup> years, which is at the lower end of typical molecular cloud lifetimes.<sup>[27]</sup>

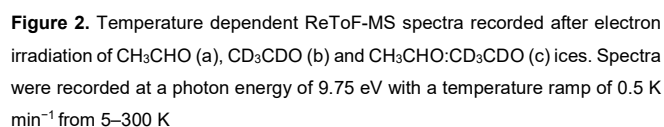
**Table 1.** Overview of experimental conditions

Ice	Thickness (nm)	Current (nA)	Irradiation time (s)	Dose (eV molecule <sup>-1</sup> )
CH <sub>3</sub> CHO	800 ± 100	40 ± 1	1800	4.7 ± 0.7
CD <sub>3</sub> CDO	800 ± 100	40 ± 1	1800	5.1 ± 0.8
mixture	900 ± 100	20 ± 1	900	1.2±0.1/1.3±0.1

**Infrared Spectroscopy.** The infrared spectra of isotopically pure ices of CH<sub>3</sub>CHO and CD<sub>3</sub>CDO before and after irradiation with energetic electrons are shown in Figure 1. Before the irradiation (black line), all absorptions can be linked to the infrared active modes of acetaldehyde and acetaldehyde-d<sub>4</sub>, respectively. Both spectra are dominated by the C=O stretching mode ( $\nu_4$ ; 1726 and 1709 cm<sup>-1</sup>, respectively). All absorptions identified prior to the irradiation are summarized in table S1 for acetaldehyde and in table S2 for acetaldehyde-d<sub>4</sub>. First, after the irradiation (red line), several new absorptions arose in the spectra. In the CH<sub>3</sub>CHO ice, carbon monoxide can be identified by its CO stretch ( $\nu_1$ ; 2129 cm<sup>-1</sup>) and methane (CH<sub>4</sub>) by its CH deformation mode ( $\nu_4$ ; 1304 cm<sup>-1</sup>). Additionally, the acetyl (CH<sub>3</sub>CO) radical at 1843 cm<sup>-1</sup> is evident from the spectrum.<sup>[28]</sup> Apart from the OH stretching region (3600–3200 cm<sup>-1</sup>), which does not allow identification of individual molecules, no evidence of vinyl alcohol is found in the IR spectra of irradiated acetaldehyde. Second, due to overlap with IR peaks of acetaldehyde-d<sub>4</sub>, neither carbon monoxide nor methane-d<sub>4</sub> (CD<sub>4</sub>) can be identified after irradiation of the CD<sub>3</sub>CDO ice. An absorption at 1577 cm<sup>-1</sup> could be linked to the (C=C) stretching mode of vinyl alcohol-d<sub>4</sub>.<sup>[29]</sup> However, this assignment cannot be confirmed in the CH<sub>3</sub>CHO, where a very strong (C=C) stretching mode was reported at 1662 cm<sup>-1</sup> for vinyl alcohol which does not overlap with any other features in the infrared spectra of the irradiated CH<sub>3</sub>CHO. Furthermore, the acetyl-d<sub>3</sub> radical (CD<sub>3</sub>CO)



**PI-ReToF-MS.** Three C<sub>2</sub>H<sub>4</sub>O isomers are clearly distinguishable through their adiabatic ionization energies (IE). Therefore, vinyl alcohol (*IE* = 9.17 eV (*syn*) / 9.30 eV (*anti*)<sup>[31]</sup>) can be unambiguously identified by using a photon energy of 9.75 eV for photoionization; neither ethylene oxide (c-C<sub>2</sub>H<sub>4</sub>O; *IE* = 10.56 eV<sup>[32]</sup>) nor acetaldehyde (*IE* = 10.229 eV<sup>[32]</sup>) can be ionized at this energy. The temperature-dependent mass spectra for all three ices are shown in Figure 2 to provide an overview of all molecules with ionization energies below 9.75 eV that formed in the experiment. Tentative assignments of molecules to major signals in the mass spectrum are given in table S3. A detailed look into the formation of vinyl alcohol in the different ices is provided in Fig.3, which shows the desorption profiles for isotopologues of vinyl alcohol, i.e. the temperature versus the intensity of the ion count(s). Comparing vinyl alcohol in pure acetaldehyde ice (Fig. 3a)) with vinyl alcohol-d<sub>4</sub> in acetaldehyde-d<sub>4</sub> ice (Fig. 3b)) it is immediately evident that despite identical experimental conditions substantially less acetaldehyde-d<sub>4</sub> is formed. Quantitatively spoken, based on the ion counts, the ratio of vinyl alcohol to vinyl



.alcohol-d<sub>4</sub> is determined to be (3.11±0.03):1 under the premise of no significant isotope effect in the ionization cross sections. This kinetic isotope effect could indicate intramolecular enolization by the [1,3]H-shift of acetaldehyde, which could still be isotope-dependent despite the high electron energy used. Previous studies employing 5 keV electrons have demonstrated that low-lying electronic states can be accessed by secondary effects, such as low-energy electrons.<sup>[33-34]</sup> Moreover, a computational analysis of hydrogen shifts demonstrated that tunneling can still be the dominant contributor to the reaction rate at temperatures well above the crossover temperature, leading to a strong kinetic

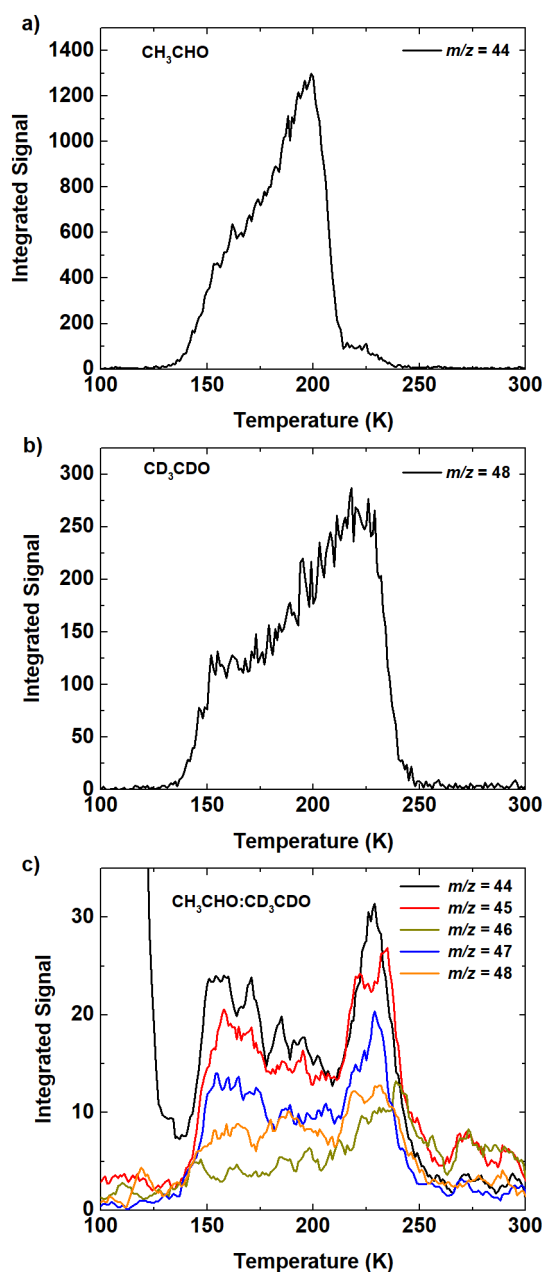
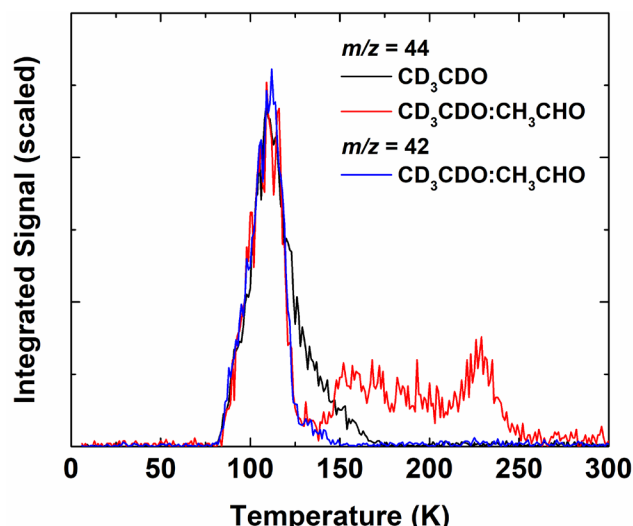


**Figure 3.** TPD profiles of different isotopologues of vinyl alcohol. a): Vinyl alcohol after irradiation of acetaldehyde. b): Vinyl Alcohol- $d_4$  after irradiation of acetaldehyde- $d_4$ . c): Vinyl alcohol with different levels of deuteration after irradiation of mixed acetaldehyde - acetaldehyde- $d_4$  ice. Spectra were recorded at 9.75 eV to exclude contributions of acetaldehyde and ethylene oxide.

isotope effect even when tunneling is energetically not required.<sup>[35]</sup>

Additional mechanistic insights into the formation of vinyl alcohol can be obtained by inspecting the distinct levels of deuteration of the vinyl alcohol formed in the ice mixture (Fig. 3c)). Ions of all possible mass-to-charge ratios for vinyl alcohol isotopologues are detected. As shown in Figure 4, the intense signal for  $m/z = 44$  at lower temperatures is due to ketene- $d_2$  and



therefore not relevant to the discussion. Most notably, vinyl alcohol- $d_1$  and vinyl alcohol are detected at similar levels and vinyl

**Figure 4.** TPD profiles of ketene- $d_2$  ( $m/z = 44$ ) in acetaldehyde- $d_4$  ices (black line) along with ketene- $d_2$  and vinyl alcohol ( $m/z = 44$ , red line), and ketene ( $m/z = 42$ , blue line) in mixed acetaldehyde - acetaldehyde- $d_4$  ice at 9.75 eV. XXX SI

alcohol- $d_3$  forms at a slightly higher abundances compared to vinyl alcohol- $d_4$ . In contrast, signal at  $m/z = 46$  (vinyl alcohol- $d_2$ ), which requires two deuterium atoms to be replaced by hydrogen or vice versa, is significantly weaker (Table 2). These findings indicate that either a significant H/D exchange between acetaldehyde and acetaldehyde- $d_4$  is taking place in the sample prior to or after intramolecular enolization or that intermolecular exchange is involved in the enolization process.

To explain the detected abundances of the aforementioned isotopologues via H/D exchange before or after enolization alone, about 50 % of all molecules would need to undergo H/D exchange. However, the infrared spectra after irradiation do not show any new absorption after irradiation that coincide with infrared features of partially deuterated acetaldehyde. Furthermore, the abundances of isotopologues of other product molecules do not agree with such an extensive H/D exchange (Table 3).

**Table 2.** Integrated ion signals and relative signal strengths of the different isotopologues of vinyl alcohol.

$m/z$	Molecular formula	Integrated Signal	Relative Signal
44	$C_2H_4O$	$1981 \pm 54$	1
45	$C_2H_3DO$	$1649 \pm 51$	$0.83 \pm 0.05$
46	$C_2H_2D_2O$	$664 \pm 35$	$0.34 \pm 0.03$
47	$C_2HD_3O$	$1132 \pm 43$	$0.57 \pm 0.04$
48	$C_2D_4O$	$886 \pm 39$	$0.45 \pm 0.03$

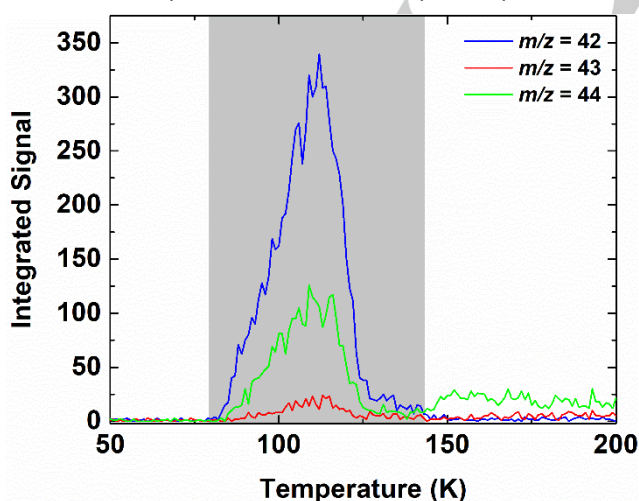
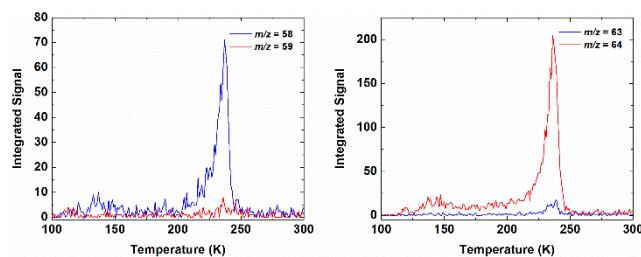
As shown here, the integrated ion signal of ketene- $d_1$  at  $m/z = 43$ , which can form from H/D exchange of either ketene or ketene- $d_2$ ,



**Table 3.** Observed ion signals associated with different isotopologues of reaction products in  $\text{CH}_3\text{CHO}:\text{CD}_3\text{CDO}$  ices.

$m/z$	Assignment	Ion Counts
42	$\text{CH}_2\text{CO}$	$7245 \pm 95$
43	$\text{CHDCO}$	$387 \pm 29$
44	$\text{CD}_2\text{CO}$	$2599 \pm 60$
58	$\text{CH}_3\text{COCH}_3$	$1110 \pm 43$
59	$\text{CH}_3\text{COCH}_2\text{D}$	$100 \pm 19$
63	$\text{CD}_3\text{COCOD}_2\text{H}$	$204 \pm 24$
64	$\text{CD}_3\text{COCOD}_3$	$3481 \pm 68$
89	$(\text{CH}_3\text{CHO})_2\text{H}^+$	$1710 \pm 270$
90	$(\text{CH}_3\text{CHO})_2\text{D}^+$	$1630 \pm 220$
91	$(\text{C}_4\text{H}_7\text{DO}_2)\text{D}^+$	$314 \pm 78$
96	$(\text{C}_4\text{D}_7\text{HO}_2)\text{H}^+$	$307 \pm 63$
97	$(\text{CD}_3\text{CDO})_2\text{H}^+$	$2053 \pm 55$
98	$(\text{CD}_3\text{CDO})_2\text{D}^+$	$2062 \pm 55$

amounts to only  $5.3 \pm 0.4 \%$  and  $15 \pm 1\%$  of that of ketene and ketene- $\text{d}_2$ , respectively (Figure 5). In the case of acetone, which forms from recombination of an acetyl ( $\text{CH}_3\text{CO}$ ) and a methyl ( $\text{CH}_3$ ) radical, acetone- $\text{d}_1$  is detected at levels of  $9 \pm 2\%$  compared to the signal of acetone; acetone- $\text{d}_5$  is formed at a fraction of only  $5.8 \pm 0.6\%$  of the ion counts of acetone- $\text{d}_6$  (Figure 6). Lastly, as previous experiments have demonstrated that the hydrogen atom of the aldehyde group is preferentially removed in the interaction with energetic electrons,<sup>[28]</sup> the protonated and deuterated dimers of acetaldehyde have also been included in table 3 to investigate product molecules with the hydrogen atom still attached to the aldehyde group. Considering that the desorption profiles of protonated and deuterated dimers overlap with those of partly deuterated dimers, their contribution to the overall signal at a given mass-to-charge ratio was determined by fitting the contributions of the two different molecules using a split Pearson VII function in the peak fitting program fity.<sup>[36]</sup> To deconvolute the individual contributions, the signal at  $m/z = 88$  ( $(\text{CH}_3\text{CHO})_2$ ) was used to find the fitting parameters for the desorption of acetaldehyde dimers; ion counts at  $m/z = 98$  ( $(\text{CD}_3\text{CDO})_2\text{D}^+$ ) were fitted to find the parameters for the desorption of protonated and

**Figure 5.** Recorded signal of isotopologues of ketene. The shaded area indicates the integration area used to exclude contribution of vinyl alcohol at  $m/z = 44$ .**Figure 6.** Recorded ion signals of different isotopologues of acetone. Left: Acetone (blue line) and acetone- $\text{d}_1$  (red line). Right: Acetone- $\text{d}_5$  (blue line) and acetone- $\text{d}_6$  (red line).

deuterated dimers. Keeping all parameters but the height of the peak fixed, these fit functions were then exploited to fit the data of the remaining mass channels where significant overlap of both signals occurred.

Figure 7 reveals the resulting fits of all mass-to-charge ratios relevant to determining the isotopic impurities of protonated and deuterated dimers. Similar ion counts are detected at mass-to-charge ratios of 89 ( $(\text{CH}_3\text{CHO})_2\text{H}^+$ ) and 90 ( $(\text{CH}_3\text{CHO})_2\text{D}^+$ ) as well as at  $m/z = 97$  ( $(\text{CD}_3\text{CDO})_2\text{H}^+$ ) and 98 ( $(\text{CD}_3\text{CDO})_2\text{D}^+$ ), indicating similar abundances of H and D atoms in the ice. A comparison of the recorded ion counts at  $m/z = 90$  to  $m/z = 91$  and those at  $m/z = 97$  to  $m/z = 96$  indicates a maximum H/D exchange ratio of  $19 \pm 5 \%$  and  $15 \pm 3 \%$  for two acetaldehyde molecules and two acetaldehyde- $\text{d}_4$  molecules, respectively. As none of the observed ratios is compatible with a 50 % H/D exchange of the reacting acetaldehyde molecules, it can be concluded that enolization of solid acetaldehyde does not exclusively proceed *via* the extensively studied intramolecular 1,3-hydrogen shift,<sup>[37]</sup> but that either intermolecular enolization of acetaldehyde or hydrogenation of ketene is a significant contributor.

As dimers of acetaldehyde with hydrogen bonding between the oxygen atoms and the methyl groups of two acetaldehyde molecules are stable,<sup>[38-39]</sup> these dimers could lead to the formation of two vinyl alcohol molecules by intermolecular hydrogen exchange. A similar pathway to enolization of acetaldehyde has previously been described in water-assisted enolization of acetaldehyde.<sup>[40]</sup> This reaction was calculated to proceed *via* a transition state that is comprised of two water molecules and one acetaldehyde molecule with hydrogen bonding between the water molecules and both a methyl hydrogen and the oxygen atom of the acetaldehyde. Furthermore, the gas-phase formic acid-catalyzed tautomerization of acetaldehyde and vinyl alcohol was calculated to proceed through

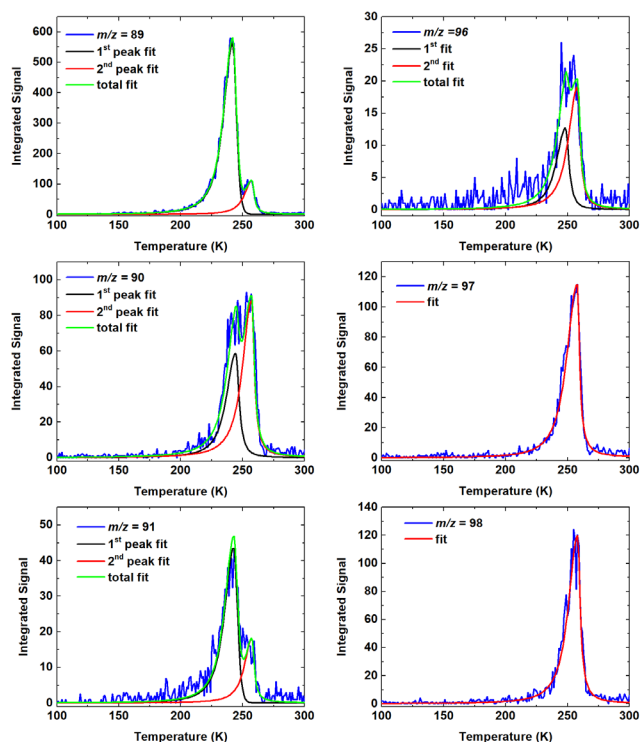


**Figure 7.** Signals associated with protonated and deuterated dimers (red fit) and dimers of isotopologues of acetaldehyde (black fit) in mixed  $\text{CH}_3\text{CHO}:\text{CD}_3\text{CDO}$  ices

a similar hydrogen bonded complex with hydrogen bonds between the formic acid and the methyl group and the oxygen atom of the acetaldehyde.<sup>[41]</sup> Therefore, intermolecular hydrogen exchange in a hydrogen-bonded dimer of acetaldehyde appears to be a plausible enolization pathway.

However, the unusually high ion counts for vinyl alcohol- $\text{d}_2$  cannot be explained by the previously discussed enolization mechanisms. The efficient formation of this isotopologue could be explained by ketene hydrogenation. As two H or D atoms are needed for this reaction, addition of two hydrogen atoms to ketene- $\text{d}_2$  or two deuterium atoms to ketene can lead to the formation of this isotopologues. The presence of several hydrogen deficient species and radicals in the sample clearly indicate that atomic hydrogen and deuterium are abundant in the sample. Nonetheless, such secondary reactions typically do not contribute significantly to the formation of reaction products at the doses employed. Indeed, the isotopologue distribution for vinyl alcohol differs significantly from this scenario: the ion signal for ketene- $\text{d}_2$  only amounts to 36% of the signal for ketene (Table 3) and the signal for the protonated and deuterated dimers indicate an equal abundance of H and D atoms in the sample. However, the relative signal for vinyl alcohol- $\text{d}_4$  is significantly higher at  $45 \pm 2\%$ . More importantly, formation of vinyl alcohol through hydrogenation of ketene would favor the formation of singly

deuterated over undeuterated, and triply deuterated over fully deuterated vinyl alcohol by a factor of 2.05 based on the abundance of the ketene isotopologues, assuming equal reaction probabilities of the isotopes. In the experiment, however, vinyl-alcohol- $\text{d}_1$  is detected at only  $83 \pm 3\%$  of vinyl alcohol and vinyl alcohol- $\text{d}_3$  is detected at  $128 \pm 8\%$  of vinyl alcohol- $\text{d}_4$ . A complete summary of the expected relative signals from ketene hydrogenation is given in Table S4. The relative underproduction of the mixed isotopologues with respect to the pure isotopologues could be accounted for by a combination of intramolecular hydrogen shift and ketene hydrogenation as primary production channel. However, the significant underproduction of vinyl alcohol- $\text{d}_2$  compared to the singly and triply deuterated vinyl alcohol suggests the previously discussed intermolecular hydrogen transfer as another significant formation channel of vinyl alcohol.

## Conclusion

Overall, taking the simple molecule acetaldehyde as prototype of an aldehyde, this study demonstrated that the enolization of aldehydes in cold molecular cloud conditions can be induced by GCRs interacting with interstellar ices. This tautomerization was found to proceed *via* three distinct pathways. The significantly lower signal in pure acetaldehyde- $\text{d}_4$  ices compared to acetaldehyde ices indicates a pathway *via* intramolecular [1,3]-H shift. Since intramolecular tautomerization *via* an [1,3]-H shift was demonstrated to easily be induced by supplying enough energy to overcome the enolization barrier in photolysis<sup>[42-43]</sup> and pyrolysis<sup>[44]</sup> experiments, it is also expected to play a major role in the GCR-induced enolization. However, the unusually high abundance of partly deuterated vinyl alcohol in mixed ices of acetaldehyde and acetaldehyde- $\text{d}_4$  cannot be explained by this enolization process alone. Relative signal strengths of different isotopologues of vinyl alcohol in mixed  $\text{CH}_3\text{CHO}:\text{CD}_3\text{CDO}$  ices suggest a second pathway *via* intermolecular hydrogen exchange in acetaldehyde dimers with hydrogen bonds between the oxygens and methyl hydrogens. A third, minor pathway inferred from the isotopic distribution is the hydrogenation of isotopologues of ketene, which produces a significant amount of doubly deuterated vinyl alcohol. Due to the low temperature, once formed and released into the gas phase in star forming regions via sublimation of the ices, where they can be detected by radio telescopes, the enols cannot overcome the tautomerization barrier. Once detected, their relative abundances can help to refine astrochemical models since they can serve as tracers for

the importance of non-equilibrium processes in the interstellar medium.<sup>[14]</sup> Furthermore, enols are important intermediates for, e.g., aldol reactions because they are nucleophiles and thus can react with electrophilic molecules such as aldehydes. Thereby, enols play a crucial role in advancing the chemical complexity in the interstellar medium and, by incorporation into comets and asteroids, in meteoric matter that can deliver prebiotic product molecules to Earth and other potentially habitable planets in exosolar systems.<sup>[45–47]</sup> Confirmation of widespread occurrence of enols in the interstellar medium can therefore help to advance our understanding of the molecular complexity found in the ISM and on comets and meteoritic samples.

## Experimental Section

Experiments were conducted in a stainless steel ultrahigh vacuum chamber at base pressures of a few  $10^{-11}$  Torr.<sup>[48]</sup> A polished  $1\text{ cm}^2$  silver substrate was interfaced to a cold head to cool it down to  $5.0 \pm 0.1\text{ K}$  using a closed cycle helium compressor (Sumitomo Heavy Industries, RDK-415E). A doubly differentially pumped rotational feedthrough (Thermionics Vacuum Products, RNN-600/FA/ MCO) in combination with a bellow allows rotation and vertical translation of the sample. Acetaldehyde (Sigma Aldrich, anhydrous  $\geq 99.5\%$  purity), and acetaldehyde- $d_4$  (Sigma Aldrich,  $\geq 99\%$  purity,  $\geq 98\text{ atom\% D}$ ) were first subjected to several freeze–thaw cycles under UHV conditions utilizing liquid nitrogen to remove residual atmospheric gases. Afterwards, impurities and acetaldehyde polymers that formed in the acetaldehyde at liquid nitrogen temperatures were removed by recondensation at  $10^{-9}$  Torr into a second glass vial submerged in an ice water bath. Acetaldehyde ices were prepared by depositing acetaldehyde vapors onto the silver substrate through glass capillary arrays at a background pressure of  $5 \times 10^{-8}$  Torr. To avoid H/D exchange prior to deposition, ice mixtures of acetaldehyde and acetaldehyde- $d_4$  were prepared by simultaneous deposition through different glass capillary arrays at partial pressures of  $2.5 \times 10^{-8}$  Torr each. The ratio of the deposited mixture was confirmed to be 1:1 by an electron impact ionization quadrupole mass spectrometer (Extrel, Model 5221) running during the TPD phase of the experiments. The integrated ion signals of the main fragments HCO ( $m/z = 29$ ) and DCO ( $m/z = 30$ ) are the same to within less than 2% (Figure S1). Thicknesses of the ices were monitored during the deposition by laser interferometry utilizing a red (632.8 nm) helium-neon laser (CVI Melles-Griot; 25-LHP-230) and a photodiode.<sup>[49]</sup>

After deposition the isotopically pure ices were irradiated with 5 keV electrons over an area of  $1.0 \pm 0.1\text{ cm}^2$  at an angle of incidence of  $70^\circ$ . Monte Carlo simulations were carried out with CASINO<sup>[50]</sup> to determine the dose each ice has received as well as the average penetration depth to ensure that the ice is sufficiently thick to prevent interaction of the silver substrate and the electrons. All relevant information about the experiments

is displayed in Table 1. The isotopic ice mixture was subjected to a lower dose to ensure that the ion signal is weak enough to not affect neighboring masses and to minimize radiation-induced H/D exchange. Infrared spectra from  $4500\text{ cm}^{-1}$  to  $500\text{ cm}^{-1}$  were taken with a resolution of  $4\text{ cm}^{-1}$  with an FTIR spectrometer (Nicolet 6700) before, during, and after irradiation to monitor changes in the composition of the ice due to the irradiation. After irradiation was complete, temperature programmed desorption was conducted by heating the sample to 300 K at  $0.5\text{ K min}^{-1}$  and subliming species were analyzed by photoionization reflectron time of flight mass spectrometry (PI-ReToF-MS), which has been described in detail previously.<sup>[51]</sup> Briefly, subliming molecules were ionized by pulsed VUV light and the ionized molecules were detected according to their arrival time in a time-of-flight spectrometer (Jordan TOF Products, Inc.).

Two synchronized Nd:YAG lasers (Spectra Physics; Quanta Ray Pro 250-30 and 270-30) were used to pump two dye lasers (Sirah Lasertechnik; Cobra-Stretch). To generate the 9.75 eV photons used in this study by four-wave mixing, the first dye laser was tuned to 606.948 nm. The laser output was frequency tripled to 202.316 nm to allow two-photon excitation of the krypton  $4s^2 4p^5 5p[1/2]_0 \leftarrow 4s^2 4p^6(^1S_0)$  resonance (101.158 nm, 12.2565 eV). The second dye laser was tuned to 495 nm (2.5 eV) and overlapped with the first beam inside a krypton jet generated by a synchronized pulsed valve operating at a backing pressure of 35 psi to generate the difference frequency between the resonance and the second laser beam. Both laser beams were focused into the gas jet using a fused silica plano convex lens (Thorlabs; LA4579;  $f = 300\text{ mm}$ ). After passing through the gas jet, the laser beams as well as the VUV light generated in the four-wave mixing process were spatially separated by an off-axis, biconvex LiF lens (ISP optics; LiF-L-31.1-3) that only allowed the VUV beam to pass through an aperture into the main UHV chamber. The beam subsequently passed the silver substrate at a distance of 1 mm to ionize subliming molecules and finally was absorbed by a Faraday cup operated at 300 V to monitor variations of the VUV flux during the experiment. Photoions were then accelerated into the time-of-flight spectrometer where they were detected by two multichannel plates in chevron configuration. The resulting signal was recorded with a multichannel scalar (FAST ComTec; P7888-1 E) operating at 30 Hz with a bin width of 4 ns and 3600 sweeps for each mass spectrum recorded, resulting in one integrated mass spectrum per Kelvin.

## Acknowledgements

Financial support from the US National Science Foundation (AST-1800975) is acknowledged. The experimental setup was financed by the W. M. Keck Foundation. N. F. K. acknowledges funding from the Deutsche Forschungsgemeinschaft (DFG, German Research Foundation) for a postdoctoral fellowship (KL 3342/1-1).

**Keywords:** IR spectroscopy • mass spectrometry • non-equilibrium processes • enolization • complex organic molecules

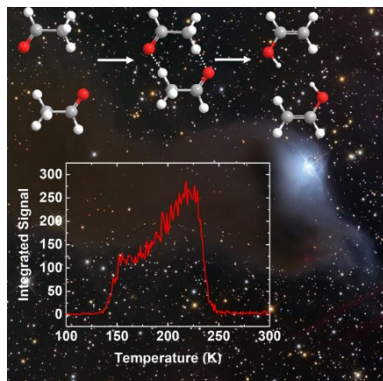


- [1] D. E. Woon, *The Astrochymist*, **2021**, available at [http://www.astrochymist.org/astrochymist\\_ism.html](http://www.astrochymist.org/astrochymist_ism.html).
- [2] R. T. Garrod, S. L. W. Weaver, E. Herbst, *Astrophys. J.* **2008**, *682*, 283.
- [3] H. M. Cuppen, C. Walsh, T. Lamberts, D. Semenov, R. T. Garrod, E. M. Penteado, S. Ioppolo, *SSRv* **2017**, *212*, 1-58.
- [4] A. Bergantini, M. J. Abplanalp, P. Pokhilko, A. I. Krylov, C. N. Shingledecker, E. Herbst, R. I. Kaiser, *Astrophys. J.* **2018**, *860*, 108.
- [5] R. I. Kaiser, S. Maity, B. M. Jones, *Angew. Chem. Int. Ed.* **2015**, *54*, 195-200.
- [6] M. P. Bernstein, S. A. Sandford, L. J. Allamandola, S. Chang, M. A. Scharberg, *Astrophys. J.* **1995**, *454*, 327.
- [7] W. Hagen, L. J. Allamandola, J. M. Greenberg, *Ap&SS* **1979**, *65*, 215-240.
- [8] M. H. Moore, B. Donn, *Astrophys. J.* **1982**, *257*, L47.
- [9] S. Maity, R. I. Kaiser, B. M. Jones, *Phys. Chem. Chem. Phys.* **2015**, *17*, 3081-3114.
- [10] F. Combes, M. Gerin, A. Wootten, G. Wlodarczak, F. Clausset, P. J. Encrenaz, *A&A* **1987**, *180*, L13-L16.
- [11] N. Fourikis, M. W. Sinclair, B. J. Robinson, P. D. Godfrey, R. D. Brown, *AuJPh* **1974**, *27*, 425-430.
- [12] J. M. Hollis, F. J. Lovas, P. R. Jewell, *Astrophys. J.* **2000**, *540*, L107.
- [13] A. M. Turner, A. S. Koutsogiannis, N. F. Kleimeier, A. Bergantini, C. Zhu, R. C. Fortenberry, R. I. Kaiser, *Astrophys. J.* **2020**, *896*, 88.
- [14] M. J. Abplanalp, S. Gozem, A. I. Krylov, C. N. Shingledecker, E. Herbst, R. I. Kaiser, *Proceedings of the National Academy of Sciences of the United States of America* **2016**, *113*, 7727-7732.
- [15] C. J. Bennett, Y. Osamura, M. D. Lebar, R. I. Kaiser, *Astrophys. J.* **2005**, *634*, 698-711.
- [16] R. L. Hudson, M. H. Moore, *Astrophys. J.* **2003**, *586*, L107-L110.
- [17] N. F. Kleimeier, A. K. Eckhardt, P. R. Schreiner, R. I. Kaiser, *Chem* **2020**, *6*, 3385-3395.
- [18] A. Mardyukov, A. K. Eckhardt, P. R. Schreiner, *Angew. Chem. Int. Ed.* **2020**, *59*, 5577-5580.
- [19] A. Mardyukov, F. Keul, P. R. Schreiner, *Chemical Science* **2020**, *11*, 12358-12363.
- [20] D. M. Mehringer, L. E. Snyder, Y. Miao, F. J. Lovas, *ApJL* **1997**, *480*, L71.
- [21] J. M. Hollis, F. J. Lovas, A. J. Remijan, P. R. Jewell, V. V. Ilyushin, I. Kleiner, *Astrophys. J.* **2006**, *643*, L25-L28.
- [22] B. E. Turner, A. J. Apponi, *Astrophys. J.* **2001**, *561*, L207-L210.
- [23] R. J. Morton, R. I. Kaiser, *P&SS* **2003**, *51*, 365-373.
- [24] P. R. Schreiner, H. P. Reisenauer, D. Ley, D. Gerbig, C.-H. Wu, W. D. Allen, *Science* **2011**, *332*, 1300.
- [25] C. J. Bennett, C. S. Jamieson, Y. Osamura, R. I. Kaiser, *Astrophys. J.* **2005**, *624*, 1097-1115.
- [26] A. M. Turner, R. I. Kaiser, *Acc. Chem. Res.* **2020**, *53*, 2791-2805.
- [27] A. Yeghikyan, *Ap* **2011**, *54*, 87-99.
- [28] N. F. Kleimeier, A. M. Turner, R. C. Fortenberry, R. I. Kaiser, *ChPhC* **2020**, *21*, 1531-1540.
- [29] M. Hawkins, L. Andrews, *J. Am. Chem. Soc.* **1983**, *105*, 2523-2530.
- [30] R. I. Kaiser, S. Maity, B. M. Jones, *Phys. Chem. Chem. Phys.* **2014**, *16*, 3399-3424.
- [31] G. Y. Matti, O. I. Osman, J. E. Upham, R. J. Suffolk, H. W. Kroto, *JESRP* **1989**, *49*, 195-201.
- [32] S. G. Lias, "Ionization Energy Evaluation" in *NIST Chemistry Webbook, NIST Standard Reference Database Number 69*, National Institute of Standards and Technology.
- [33] L. Zhou, R. I. Kaiser, L. G. Gao, A. H. H. Chang, M. C. Liang, Y. L. Yung, *Astrophys. J.* **2008**, *686*, 1493-1502.
- [34] N. F. Kleimeier, M. J. Abplanalp, R. N. Johnson, S. Gozem, J. Wandishin, C. N. Shingledecker, R. I. Kaiser, *Astrophys. J.* **2021**, *911*, 24.
- [35] M. Kryvohuz, *J. Phys. Chem. A* **2014**, *118*, 535-544.
- [36] M. Wojdyr, *JApCr* **2010**, *43*, 1126-1128.
- [37] B. J. Smith, M. T. Nguyen, W. J. Bouma, L. Radom, *J. Am. Chem. Soc.* **1991**, *113*, 6452-6458.
- [38] T. S. Thakur, M. T. Kirchner, D. Bläser, R. Boese, G. R. Desiraju, *Phys. Chem. Chem. Phys.* **2011**, *13*, 14076-14091.
- [39] J. M. Hermida-Ramón, M. A. Ríos, *Chem. Phys. Lett.* **1998**, *290*, 431-436.
- [40] S. Yamabe, N. Tsuchida, K. Miyajima, *J. Phys. Chem. A* **2004**, *108*, 2750-2757.
- [41] J. Peeters, V. S. Nguyen, J.-F. Müller, *JPCL* **2015**, *6*, 4005-4011.
- [42] A. E. Clubb, M. J. T. Jordan, S. H. Kable, D. L. Osborn, *JPCL* **2012**, *3*, 3522-3526.
- [43] D. U. Andrews, B. R. Heazlewood, A. T. Maccarone, T. Conroy, R. J. Payne, M. J. T. Jordan, S. H. Kable, *Science* **2012**, *337*, 1203.
- [44] A. K. Vasiliou, K. M. Piech, B. Reed, X. Zhang, M. R. Nimlos, M. Ahmed, A. Golan, O. Kostko, D. L. Osborn, D. E. David, K. N. Urness, J. W. Daily, J. F. Stanton, G. B. Ellison, *J. Chem. Phys.* **2012**, *137*, 164308.
- [45] G. Cooper, N. Kimmich, W. Belisle, J. Sarinana, K. Brabham, L. Garrel, *Nature* **2001**, *414*, 879-883.
- [46] G. Cooper, C. Reed, D. Nguyen, M. Carter, Y. Wang, *PNAS* **2011**, *108*, 14015.
- [47] M. J. Mottl, B. T. Glazer, R. I. Kaiser, K. J. Meech, *Geoch* **2007**, *67*, 253-282.
- [48] B. M. Jones, R. I. Kaiser, *JPCL* **2013**, *4*, 1965-1971.
- [49] A. M. Turner, M. J. Abplanalp, S. Y. Chen, Y. T. Chen, A. H. H. Chang, R. I. Kaiser, *Phys. Chem. Chem. Phys.* **2015**, *17*, 27281-27291.
- [50] D. Drouin, A. R. Couture, D. Joly, X. Tastet, V. Aimez, R. Gauvin, *Scanning* **2007**, *29*, 92-101.
- [51] M. J. Abplanalp, M. Förstel, R. I. Kaiser, *Chem. Phys. Lett.* **2016**, *644*, 79-98.



## Entry for the Table of Contents

Insert graphic for Table of Contents here.



Secondary electrons from galactic cosmic rays can induce the enolization of acetaldehyde in the solid state.

Institute and/or researcher Twitter usernames: @UHMRxnDynamics